Predicting Electromigration Mortality Under Temperature and Product Lifetime Specifications

Vivek Mishra and Sachin S. Sapatnekar
Department of Electrical and Computer Engineering,
University of Minnesota, Minneapolis, MN 55455
{vivek,sachin}@umn.edu*

ABSTRACT

Today's methodologies for electromigration (EM) identify EM-susceptible wires based on their current density, using the Blech criterion to filter out wires that are EM-immortal. The Blech criterion is agnostic to the product lifetime and temperature conditions: many Blech-mortal wires may never experience EM during the product lifetime. We develop new methods that evaluate the transient evolution of stress, relative to the product lifetime, and present an improved set of simple and practical mortality criteria. On a set of power grid benchmarks, we demonstrate that the actual number of mortal wires may depend strongly on the lifetime and reliability conditions.

Keywords

Electromigration, Blech length, steady state, stress

1. INTRODUCTION

Technology scaling has resulted in a monotonic increase in the current density, causing electromigration (EM) in interconnects to be a major concern [1]. As EM considerations become more critical, there is a need for circuit analysis and design techniques to incorporate the knowledge of EM reliability physics to realize a design which meets the expected performance as well as the reliability targets.

Today's signoff flows [2] first filter out EM-immortal wires based on Blech criterion [3], which compares the jL product, of the length L and current density j of a wire, against a threshold value: if this threshold is not exceeded, the wire is immortal. For the remaining wires, a current density limit, based on Black's equation [4], is applied to check mortality.

In this work, we perform a rigorous analysis of the dynamics of EM stress evolution to provide concrete product-lifetime-specific criteria for mortality. Figure 1 shows the stress evolution for a wire with length, $L = 100\mu\text{m}$, which is carrying a current density $j = 0.5\text{MA/cm}^2$ at an operating temperature $T = 105°\text{C}$. We use the process parameters corresponding to modern Cu Dual Damascene (Cu DD) based technology, listed in Table 1. For a product lifetime of 5 years, the wire is immortal, since the stress does not cross the critical stress, σ_c, in this interval. For a 20-year lifetime, the same wire is mortal since its stress crosses σ_c.

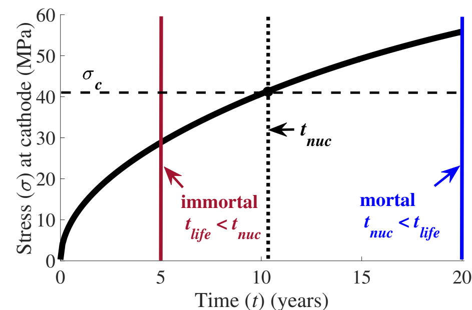

Figure 1: Wire mortality and product lifetime.

Most designers realize that compared to long-lifetime (e.g., automotive) parts, products with shorter lifetimes (e.g., mobile clients) should have fewer EM-susceptible mortal wires. The Blech criterion is inherently unable to capture lifetime considerations because it is valid only for wires that achieve steady state [5, 6], and it does not consider transient EM behavior. While the current density check based on Black's equation [4] is lifetime-dependent, it is limited due to its simple and empirical nature: it does not capture the dependence on all process parameters [7], and its current density limit is the same for all wires, and cannot capture the dependence of EM on wire length [8].

The idea of comparing the nucleation time with lifetime to determine mortality has been introduced in [9], and also addressed in [10], but their analysis is simpler and less rigorous than our approach. Unlike [9] and [10], we concretely incorporate the effects of line lengths, which can be significant. The Blech criterion also predicts immortality, but it is based on a steady state, and unlike our work, does not consider the transient, which can be long. The work in [11] proposes an approximate physics-based model, but it relies on the Blech criterion, and as shown in Section 3.2, its approximate truncation for finite lines incurs significant errors for medium to long wires.

We present a new criterion that accounts for the role of product lifetime and temperature in determining wire mortality for a given set of process parameters. Our criterion for mortality analyzes the stress evolution in the interconnect. This work presents a method that overcomes *all* of the disadvantages listed above: it is accurate, valid over a range of wire lengths, does not assume steady state and includes the transient, and is physics-based rather than empirical.

*This work was partially supported by the NSF awards CCF-1421606, CCF-1162267, and the Doctoral Dissertation Fellowship, University of Minnesota. The authors acknowledge the Minnesota Supercomputing Institute (MSI) at the University of Minnesota for providing resources that contributed to the research results reported within this paper.

Permission to make digital or hard copies of all or part of this work for personal or classroom use is granted without fee provided that copies are not made or distributed for profit or commercial advantage and that copies bear this notice and the full citation on the first page. Copyrights for components of this work owned by others than ACM must be honored. Abstracting with credit is permitted. To copy otherwise, or republish, to post on servers or to redistribute to lists, requires prior specific permission and/or a fee. Request permissions from permissions@acm.org.

DAC '16, June 05-09, 2016, Austin, TX, USA
© 2016 ACM. ISBN 978-1-4503-4236-0/16/06…$15.00
http://dx.doi.org/10.1145/2897937.2898070

2. BACKGROUND: EM MODELING

EM-induced degradation in Cu interconnects occurs due to the nucleation and growth of voids [6,12]. As the void grows, it results in an increase in the wire resistance, which ultimately causes functional failure. As the current flows in the interconnect, atoms move in the direction of electron flow, creating a tensile stress near the cathode and a compressive stress near the anode. This resulting stress gradient causes the generation of a back-stress force in the wire.

Figure 2 illustrates the two driving forces – the electron wind force, due to the current flow, and the back-stress force, which is generated as a result of the stress gradient generated due to EM-induced mass redistribution. As the movement of migrated atoms is blocked at either end due to the atom-impermeable Ta barrier layer, the electron wind force results in atomic depletion at the cathode, resulting in a tensile stress generation at the cathode. At the anode, the migrated atoms accumulate, creating a compressive stress. As a result, voids tend to form at the cathode. In principle, voids may form either inside the via or along the line. However, process advances using improved liner deposition [13] virtually remove the possibility of voids inside the via.

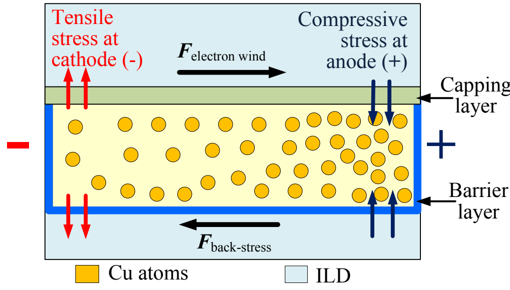

Figure 2: Cross section of a Cu wire indicating the back-stress and the electron wind force.

The temporal evolution of EM-induced stress involves the interaction between electron wind and back-stress. This is modeled by the partial differential equation [14]

$$\frac{\partial \sigma}{\partial t} = \frac{\partial}{\partial x}\left[\kappa\left(\frac{\partial \sigma}{\partial x} + G\right)\right] \tag{1}$$

Here, the part involving G corresponds to the electron wind force and the one including $\frac{\partial \sigma}{\partial x}$ represents the back-stress force. Other terms are defined as: $\kappa = \frac{D_{\mathit{eff}}\, B\, \Omega}{k_B T}$, $G = \frac{eZ^{\star}_{\mathit{eff}}\, \rho\, j}{\Omega}$, D_{eff} is the EM effective diffusivity, given by $D_{\mathit{eff}} = D_0 \exp\left(-E_a/k_B T\right)$, where D_0 is the diffusivity constant, E_a is the activation energy, k_B is Boltzmann's constant, T is the temperature, e is the elementary electron charge, B is the effective bulk modulus for the metal-ILD system, Ω is the atomic volume for the metal, $Z^{\star}_{\mathit{eff}}$ the effective charge number, and ρ is the resistivity. The partial derivatives are with respect to x, the distance from the cathode, and time, t.

2.1 Traditional EM modeling

The conventional method for EM analysis for interconnects involves a two-step process. The first step involves filtering out EM immortal wires using the Blech criterion [3]. Mortal wires are susceptible to EM and can potentially cause EM failure. In the second step, the current density flowing through these wires is checked against a global limit, which is determined using the Black's equation [4].

2.1.1 *The Blech criterion*

The work in [3] observed that for a certain range of current and wire length combinations, the wire is immune to EM degradation if the product of the current density through the wire, j, and the wire length, L is below a threshold. For these wires, no EM-induced damage occurs because an equilibrium between the back-stress force and the electron wind force is accomplished. This steady state is reached once the two forces balance, and no further net EM-induced atomic flow occurs. The stress does not change with time after the achievement of the steady state, i.e., $\frac{\partial \sigma}{\partial t} = 0$.

Using the above condition in (1) along with the assumption that there is no initial stress at time $t = 0$ implies that

$$\frac{\partial \sigma}{\partial x} + G = 0 \tag{2}$$

For a constant current flow (i.e., constant G), the slope of the stress profile at steady state is a constant, i.e.,

$$\left|\frac{\partial \sigma}{\partial x}\right| = \left|\frac{\Delta \sigma}{L}\right| = G \tag{3}$$

At **steady state**, the stress gradient at the cathode is $\frac{\Delta\sigma}{L} = \frac{2\sigma}{L}$ [6]. If the tensile stress at steady state is smaller than the critical stress, σ_c, the wire will be literally immortal to EM damage, for all time, i.e., the stress $\sigma < \sigma_c$. Using the above relations, along with (3), we obtain

$$G = \frac{2\sigma}{L} \leq \frac{2\sigma_c}{L} \tag{4}$$

$$\implies \frac{eZ^{\star}_{\mathit{eff}}\, \rho\, j}{\Omega} \leq \frac{2\sigma_c}{L} \tag{5}$$

$$\implies (j\ L) \leq \frac{2\sigma_c \Omega}{eZ^{\star}_{\mathit{eff}}\, \rho} = (j\ L)_{\text{crit}} \tag{6}$$

This is the threshold used in the Blech criterion. Conversely, the wire mortality condition can be written as

$$j\ L \geq (j\ L)_{\text{crit}} \tag{7}$$

Despite the simplicity of the Blech criterion, one of its limitations is that it is based on the assumption that a steady state is achieved between the electron wind and back-stress.

However, recent Cu DD process enhancements for performance improvement may challenge the above assumption. Recent technology upgrades, such as the introduction of low-k interlayer dielectric (ILD), and usage of ultra-thin Ta barrier layer has resulted in lower back-stress compared to earlier interconnect technologies [5, 8]. This can result in an increase in the time required for sufficient mass transfer to generate a back-stress to balance the electron wind force [15]. For some wires, the time to steady state may surpass the product lifetime, and the Blech criterion may estimate the stress at a time later than the circuit lifetime.

2.1.2 *Black's equation*

Wires that are rendered mortal by the Blech criterion need further analysis to check if they can use EM damage during the lifetime of the product. This is done using the Black's equation [4], which describes the mean time to failure, $MTTF$ for a wire under EM as

$$MTTF = \frac{A}{j^n} \exp \frac{E_a}{k_B T} \tag{8}$$

Here, A and n are constants and typical values of n are between 1 and 2. Industry practice involves setting up a current density limit using the above equation for a given

target $MTTF$. The issue with using a current density limit derived from (8) has to do with its empirical nature, which does not capture the impact of some EM related circuit and process parameters. Moreover, the value of the exponent n, is a matter of controversy for Cu DD interconnects [7].

Further, the current density limit imposed is not context-dependent, but is identical for all wires. Experiments show that short and long wires show different EM characteristics due to the role of mechanical properties [8].

3. TRANSIENT STRESS MODELING

For modern interconnect Cu interconnects, steady state may not be achieved during the product lifetime. We check for EM-susceptibility based on the evolution of stress as a function of time. For our analysis, we are interested in the general solution for stress evolution. We will discuss the two solutions relevant to our analysis, corresponding to the two cases – a semi-infinite (SI) line and a finite (F) line as described in [14]. The cathode for the line is at $x = 0$ in both cases; for the semi-infinite case, the anode is at ∞, while for the finite line, the anode is at a finite $x = L$.

For each case, the solution is based on the boundary condition that the net atomic flux at the endpoints enclosed by vias is zero. The zero flux at an interconnect endpoint occurs because the Ta barrier at the vias in a Cu DD process blocks the flow of metal atoms. The zero flux boundary conditions (BC) for each of these two scenarios are given as

$$BC_{SI} : \frac{\partial \sigma}{\partial x} + G = 0, \text{ at } x = 0, \text{ for all } t \tag{9}$$

$$BC_{F} : \frac{\partial \sigma}{\partial x} + G = 0, \text{ at } x = 0, x = L, \text{ for all } t \tag{10}$$

3.1 Stress evolution at cathode

For copper interconnects voids typically form near the cathode [16], and the stress evolution at the cathode ($x = 0$) is of primary interest. The stress solutions at $x = 0$ are [14]

$$\sigma_{SI}(0,t) = 2G\sqrt{\frac{\kappa t}{\pi}} \tag{11}$$

$$\sigma_{F}(0,t) = GL\left(\frac{1}{2} - 4\sum_{n=0}^{\infty}\frac{e^{-m_n^2\,\frac{kt}{L^2}}}{m_n^2}\right) \tag{12}$$

where $m_n = (2n + 1)\pi$. The solution for the SI boundary condition is compact, and thus useful in circuit analysis [9, 17]. However, σ_{SI} is pessimistic since the SI case experiences lower back-stress. Moreover, the SI model has no length dependence since the wire has infinite length.

For wires in power grids, the length, L, may vary from a scale of micrometers to hundreds of micrometers. The solution corresponding to the finite line BC is a realistic choice, since it directly models the length dependency. However, the finite wire solution, σ_F, includes an infinite series, which makes its exact evaluation computationally difficult.

3.2 Analysis: Semi-infinite and finite line model

Figure 3 shows the stress as a function of time, for the SI and F cases, for two values of wire length, $L = 50\mu$m and 75μm. The current density used for the above simulation, $j = 0.5\text{MA/cm}^2$. The process parameters along with the sources are listed in Table 1. It can be seen that the solutions for the SI and F cases differ for $L = 50\mu$m (as shown in Figure 3(a)), and the differences reduce for a larger value of $L = 75\mu$m, as shown in Figure 3(b). Notice that the two solutions begin to diverge after an initial period. The work in [14] observes that the steady state for a line of length, L, can be achieved in time $t \approx \frac{L^2}{4\kappa}$, and we can observe that at this instant the stress prediction between the two lines can differ significantly. However, we observe that the two solutions do not differ significantly, during initial stages up to $t = 5$ years for both cases. This is because sufficient back-stress has not built up during this time.

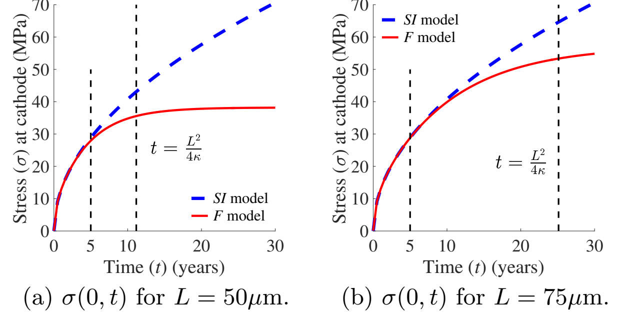

(a) $\sigma(0,t)$ for $L = 50\mu$m. (b) $\sigma(0,t)$ for $L = 75\mu$m.

Figure 3: Stress at the cathode, as predicted by SI and F model at multiple wire length, L.

To predict the wire mortality as a function of the product lifetime, we use the formulation for stress at the cathode in the SI line, as in (11), and the F line, as in (12).

In fact, the solution corresponding to the semi-infinite line, σ_{SI}, shown in (11) is an upper bound on σ_F, which is also observed in Figure 3. This occurs because a finite line sees a larger back-stress than the semi-infinite line, and the larger back-stress attenuates the net stress at the cathode. This larger back-stress is a result of a larger stress gradient compared to the semi-infinite line. The implication of this observation is that if the stress predicted by the SI solution shown in (11) is less than the critical value, σ_c, *the wire is sure to be immortal.* In this case, we do not need to evaluate the more accurate stress using the F solution shown in (12), which involves the evaluation of an infinite series.

Additionally, for the solution corresponding to the finite line σ_F in (12), we study the variation in the error in predicting σ_F by considering truncation of the infinite series for multiple values of n, for multiple wire length, L. The accurate stress corresponds to the truncation at $n = 100$.

The analysis in [11] truncates the series to only one term, corresponding to $n = 0$. For $L = 100\mu$m, Figure 4(a) shows that such a truncation does not differ from the accurate solution. In contrast, for $L = 300\mu$m, Figure 4(b) demonstrates that the stress computed by the $n = 0$ truncation leads to significant deviation from the correct value. The truncated sum converges as the number of terms increases from $n = 0$ to $n = 4$, and the plots corresponding to $n = 4$ matches the accurate solution. We choose a value of $n = 20$ to cover the range of wire length up-to a worst-case limit of 2000μm and a worst-case current density of 3MA/cm^2. We use the process parameters from Table 1. For a different process, the number of terms may be determine through a single characterization for the longest wire length.

For this technology, for wire lengths larger than 100μm, the solution corresponding to the semi-infinite line (SI) closely matches the numerical solution corresponding to the finite line (F). This is also indicated by observing the reduction in the difference between stress prediction using the SI and F models as the wire length increases, as shown in Figure 3.

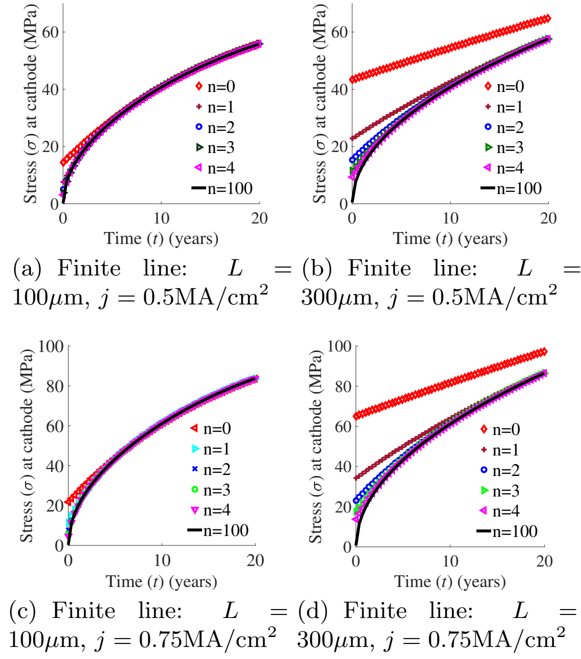

(a) Finite line: $L = 100\mu$m, $j = 0.5$MA/cm^2 (b) Finite line: $L = 300\mu$m, $j = 0.5$MA/cm^2

(c) Finite line: $L = 100\mu$m, $j = 0.75$MA/cm^2 (d) Finite line: $L = 300\mu$m, $j = 0.75$MA/cm^2

Figure 4: Finite line model prediction, for different values of n in (12), at multiple scenarios of j, L.

3.3 Hierarchical mortality criteria

We discuss our framework, which uses the previous observations to predict wire mortality in power grid. We take as input the current density j and the length L for every wire, and the process and environment specifications. The output of our framework is the set of EM-susceptible wires. Note that we use "mortal" and "EM-susceptible" as synonyms.

As shown in the schematic in Figure 5, our framework sequentially filters out wires that are immortal stage-by-stage in order to reduce the number of candidates for the finite wire model F, since it is the most computation intensive by virtue of its structure as it involves computation of nonlinear series involving wire length, L.

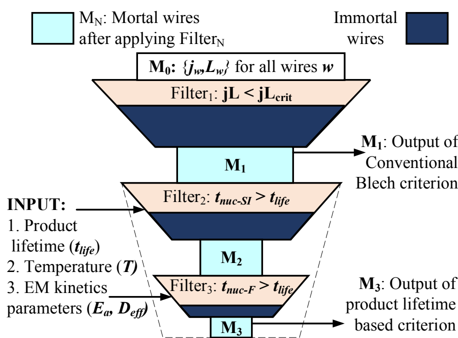

Figure 5: Sequential filtering of mortal wires.

We sequentially use the Blech criterion, the semi-infinite line (SI) solution (11), and the finite line (F) solution (12). This enables us to tackle the trade-off between the limited accuracy and lifetime-independence of the easy to compute Blech-criterion, against the more accurate, but computation intensive finite line formula. We now discuss the three stages utilized to filter out the immortal wires in order to obtain the final, realistic estimate for the number of mortal wires corresponding to the lifetime, and process specifications.

Filter 1: We first use the Blech criterion discussed in Section 2.1.1 to filter out wires that are immortal under any product lifetime. The Blech criterion is based on the peak stress achievable, and if this never crosses the critical stress, σ_c, then the wire is immortal regardless of lifetime.

Filter 2: Next, for the remaining wires, we obtain an optimistic estimate of the nucleation time, t_{nuc-SI} by using (11) to solve for the time at which the stress at the cathode reaches the critical stress, i.e., $\sigma_{\rm SI}(0, t_{nuc-SI}) = \sigma_c$, i.e.,

$$t_{nuc-SI} = \frac{\pi \, \sigma_c^2}{4 \, G^2 \, j^2 \, \kappa} \tag{13}$$

The estimate is optimistic because the actual stress is at most σ_{SI}, and the actual value of t_n is no smaller than the value predicted here. Therefore, any wire for which the estimated $t_{nuc-SI} > t_{life}$ also has the property that its real nucleation time $t_n > t_{life}$, i.e., it is effectively immortal.

Filter 3: For the remaining wires, the actual nucleation time may or may not exceed the product lifetime. For these potentially mortal wires, we compute the precise nucleation time, t_{nuc-F}, for the wire by numerically solving the stress expression in (12), truncated to 20 terms, to solve for t_{nuc-F}

$$\sigma_F(0, t_{nuc-F}) = \sigma_c \tag{14}$$

using a Newton-Raphson approach. If the final value of t_{nuc-F}, as predicted by our iterative procedure, exceeds the product lifetime, t_{life}, then the wire is effectively immortal.

As indicated previously, the first two criteria are simple to evaluate and involve closed-form expressions. The last criterion requires a numerical procedure to solve (12). This step involves more (but manageable) computation than the first two criteria, but applied to a smaller set of wires that are not already eliminated as immortal by the previous criteria.

4. RESULTS

We implement our method described in Section 3.3, using `MATLAB` and `C++`, and we test our analysis on a set of standard power grid circuits to estimate the number of mortal wires as a function of the product lifetime for a set of temperature and Cu DD process specifications, listed in Table 1.

Symbol	Definition	Value
ρ	Resistivity	2.25×10^{-8}Ohm-m
Ω	Atomic volume	1.18×10^{-29} m^3
B	Effective bulk modulus	28GPa [17]
σ_c	Critical stress	41MPa [17]
$Z^\star_{eff}$	Atomic charge number	1 [17]
D_0	Diffusivity constant	1.3×10^{-9}m^2/s [17]
E_a	Activation energy	0.8eV [17]

Table 1: EM process parameters for Cu DD interconnects.

The power grid circuits used in our simulations are a set of industrial benchmarks imported from [18]. Note that the percentage nominal IR drop, defined as the worst IR drop value among all the nodes as a percentage of supply voltage at time $t = 0$, was unrealistically high in some of the original benchmarks ($> 20\%$), and is scaled in a similar manner as discussed in [11], we have scaled the original value of current loads for these benchmarks, such that the percentage nominal IR drop is in the 11-12% range for all the circuit benchmarks.

We take as input the process parameters, corresponding to the Cu DD technology from Table 1, along with the current density and wire length for every wire.

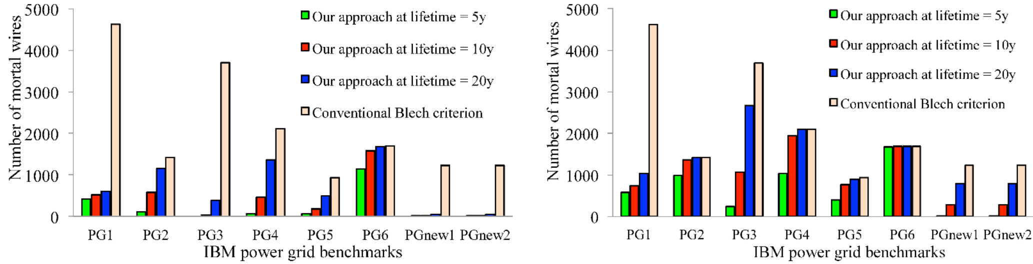

(a) Number of mortal wires at $T = 105°$C. (b) Number of mortal wires at $T = 125°$C.

Figure 6: Mortal wires: Conventional Blech criterion vs.òur product lifetime based approach.

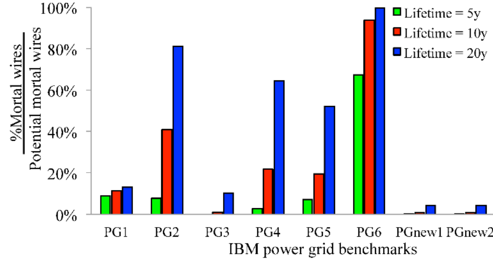

(a) % Mortal wires at $T = 105°$C.

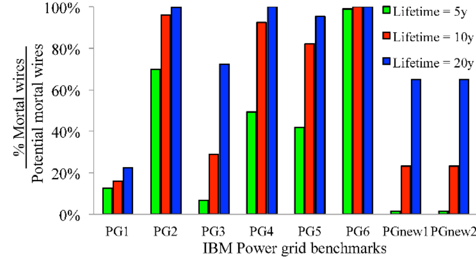

(b) % Mortal wires at $T = 125°$C.

Figure 7: Mortal wires expressed as a percentage of the potential mortal wires predicted by the conventional Blech criterion.

Comparison with Blech: Figure 6 shows the number of mortal wires as predicted by our approach at multiple product lifetime values of 5, 10, and 20 years, representing the mobile, computing, and automotive application lifetime values. We compare our prediction against the classical Blech criterion. We show our calculations for two values of operating temperature $T = 105°$C (Figure 6(a)) and $T = 125°$C (Figure 6(b)). We do not show wires caught by Black's equation here, but will do so later.

For all power grid circuits, the number of mortal wires from our approach is smaller or equal to the number of mortal wires predicted by the conventional Blech criterion, for each specification of product lifetime. This is not surprising because Filter 1 in our approach is the Blech criterion. Our mortal set is provably a subset of Blech-mortal wires.

The difference in the prediction between the two approaches is largest for short-lifetime (5 years) applications, and the difference reduces for larger lifetimes. This is because at smaller lifetime values, most of the wires do not undergo significant mass transfer which can generate enough stress for void nucleation. The Blech criterion, by construction bases its analysis at the time when steady state is achieved, and thereby renders some of these wires as mortal wires.

In Figure 6(b), for a fixed lifetime, the number of mortal wires is seen to increase for a larger value of temperature. This is because the transient stress characteristics are a strong function of temperature due to the Arrhenius relationship between D_{eff} and T. In contrast, the steady state characteristics in (6) are temperature independent, and that is why the number of mortal wires predicted by the conventional Blech criterion are the same for both temperatures.

Figure 7 shows the number of mortal wires as a fraction of those predicted by the Blech criterion. We observe an increase in the number of mortal wires for a larger temperature of $T = 125°$C (Figure 7(b)) as compared to $T = 105°$C (Figure 7(a)). This increase occurs over all benchmarks.

For a lifetime of 20 years, data corresponding to the power grid benchmarks: PG2, PG4, PG5, and PG6 indicates that close to 100% of the wires predicted as potentially mortal by the Blech criterion are indeed mortal by our criteria. For the remaining benchmarks, the gap between the two approaches is significant. Some of the wires predicted by Blech as mortal, are immortal even at a lifetime of 20 years. This is possibly due to the fact that power grids PG1, PG3, PGnew1, and PGnew2 have longer wires, some of the order 1000μm, in PG1. Due to the large wire length, the $j\ L$ product for these wires is large, even for a small current density value, and may cross the critical value, which renders them mortal. However, because of the low current density, the time taken for the mass transfer required for steady state will exceed the lifetime. A current density filter such as Black's equation or the Filter 2 proposed in our approach will see that this wire does not experience EM degradation, thus averting the pessimism due to the Blech criterion.

Effectiveness of each filter: Next, we observe the distribution of wires, which are filtered out after application of each of the three wire mortality filters, as described in Section 3.3. Figure 8 shows this statistic, for the benchmark circuit IBMPG2. The data is shown for different values of product lifetimes, $t_{life} = 5, 20$ years. The wire lengths are indicated on the x axis and the corresponding current density is plotted on the y axis. The plot shows the number of mortal wires as predicted by our approach, along with the wires which, although predicted as mortal by the Blech criterion (Filter 1), but are filtered out as immortal by us.

From Figure 8(b) we can observe that for a lifetime of 20 years, almost all the wires are mortal and the number of mortal wires decreases corresponding to shorter lifetime of 5 years shown in Figure 8(a). Furthermore, notice that the simple to compute Filter 2 filters out a majority of wires compared to the computation intensive Filter 3, which is in agreement with our observation in Section 3.2.

These observations highlight the pessimism in the Blech criterion and emphasize the importance of a lifetime-based mortality filter, such as the one obtained by Black's equation or ours from Section 3.3, which we show to be better.

Comparison with Blech+Black: We now compare the distribution of wires filtered out using our framework with

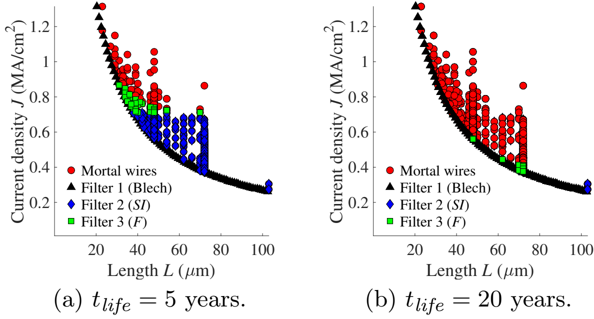

(a) $t_{life} = 5$ years. (b) $t_{life} = 20$ years.

Figure 8: Distribution of mortal wires for IBMPG2 at different lifetime, t_{life}, for $T = 105°$C

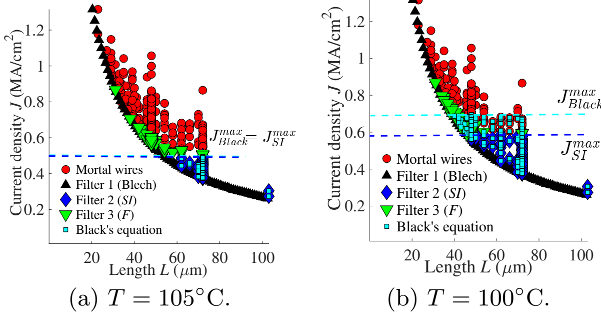

(a) $T = 105°$C. (b) $T = 100°$C.

Figure 9: Distribution of mortal wires for IBMPG2 at different temperature, T, at $t_{life} = 10$ years

the traditional current density filter derived from Black's equation. Figure 9 shows the distribution of wires filtered as immortal using our criterion and the Black's equation, for two different temperature values of $T = 105, 100°$C. The Blech filter removes many wires below the jL=constant curve and to reduce clutter, we only show the frontier of the curve in these plots. To characterize the pre-exponential constant in Black's equation, we assume that a wire with current density 0.5MA/cm^2, has a lifetime of 10 years at temperature, $T = 105°$C. This assumption enables us to have the same current density limit at $T = 105°$C, as shown by J^{max}_{Black} and J^{max}_{SI} in Figure 9(a). However, *both of these criteria miss wires (green points) that are captured only by our Filter 3.* A constant j filter would mix these green points with red mortal wires, because neither Black's equation nor our Filter 2 can fully capture the role of wire length in EM evolution.

From Figure 8(b), we observe that at a slightly smaller temperature value $T = 100°$C, the maximum current density limit as obtained using the Black's equation and our filter 2 increases. This is because of the exponential dependence of EM dynamics on temperature, which is modeled by both the above formulations. However, the jump in the current density criterion from using the Black's equation is larger than that observed by our Filter 2. This is because the pre-exponential factor in Black's equation is temperature independent in the way it is used today in industry settings. However, in reality the pre-exponential factor has a temperature dependency [7]. Our model and framework explicitly captures this temperature dependency.

Impact of process: Lastly, we perform simulations which use different specifications of process parameters corresponding to the Cu Dual Damascene interconnect technology, which are listed in Table 1 and Table 2. We perform our simulation, corresponding to two alternate Cu DD process, which are differ the Cu-capping materials used. The EM diffusion process parameters are taken from [12] and listed in Table 2. The grain size is assumed to be 0.1μm.

Cu DD Process		
Grain size = 0.1μm E_a = 0.84eV	Set I Cu/dielectric	Set II Cu/CoWP
$Z^{\star}_{eff}D_0(m^2/s)$	5×10^{-9}	4×10^{-9}

Lifetime (years)	Blech Mortal	% Mortal wires for IBMPG2 Set I	Set II
5	1418	11.6	5.3
10	1418	51.2	35.7
20	1418	84.8	73.8

Table 2: Mortal wire prediction for IBMPG2.

Notice that, the conventional Blech criterion, predicts the same number of mortal wires (=1418), for two processes. This is because the conventional criterion is oblivious to EM parameters like D_0, as they do not appear in (6) or (8). In contrast, the number of mortal wires as predicted by our work vary depending on the process parameters. Table 2 list the number of mortal wires predicted by our criterion as a percentage of the number of mortal wires predicted by the conventional Blech criterion. Notice, that for a larger value of EM diffusivity constant D_0, corresponding to process Set I, the percentage mortal wires are larger. This is intuitive, since a larger diffusivity implies faster mass transfer.

5. REFERENCES

[1] International Technology Roadmap for Semiconductors, online chapter available at http://www.itrs.net/Links/2013ITRS/2013Chapters/2013Interconnect.pdf.

[2] J. Lienig, "Electromigration and its impact on physical design in future technologies," in *Proc. ISPD*, 2013, pp. 33–40.

[3] I. A. Blech, "Electromigration in thin aluminum films on titanium nitride," *J. Appl. Phys.*, vol. 47, no. 4, pp. 1203–1208, 1976.

[4] J. R. Black, "Electromigration failure modes in aluminum metallization for semiconductor devices," *Proc. IEEE*, vol. 57, no. 9, pp. 1587–1594, 1969.

[5] E. Ogawa *et al.*, "Reliability and early failure in Cu/Oxide Dual-Damascene interconnects," *J. Electron. Mater.*, vol. 31, no. 10, pp. 1052–1058, 2002.

[6] C. S. Hau-Riege *et al.*, "The effect of interlevel dielectric on the critical tensile stress to void nucleation for the reliability of Cu interconnects," *J. Appl. Phys.*, vol. 96, no. 10, pp. 5792–5796, 2004.

[7] J. Lloyd, "Black's law revisted—Nucleation and growth in electromigration failure," *Microelectron. Reliab.*, vol. 47, no. 9, pp. 1468–1472, 2007.

[8] A. Oates and M. Lin, "The impact of trench width and barrier thickness on scaling of the electromigration short - length effect in Cu / low-k interconnects," in *Proc. IRPS*, 2013, pp. 3F.1.1–3F.1.5.

[9] V. Mishra and S. S. Sapatnekar, "The impact of electromigration in copper interconnects on power grid integrity," in *Proc. DAC*, 2013, pp. 88:1–88:6.

[10] Reference withheld, PDF provided in disclosure process.

[11] X. Huang *et al.*, "Physics-based electromigration assessment for power grid networks," in *Proc. DAC*, 2014, pp. 80:1–80:6.

[12] A. S. Oates, "Strategies to ensure electromigration reliability of Cu/Low-k interconnects at 10 nm," *ECS J. Solid State Sc.*, vol. 4, no. 1, pp. N3168–N3176, 2015.

[13] B. Li *et al.*, "Electromigration challenges for advanced on-chip Cu interconnects," *Microelectron. Reliab.*, vol. 54, no. 4, pp. 712–724, 2014.

[14] M. A. Korhonen *et al.*, "Stress evolution due to electromigration in confined metal lines," *J. Appl. Phys.*, vol. 73, no. 8, pp. 3790–3799, 1993.

[15] P. S. Ho *et al.*, "Effect of low k dielectrics on electromigration reliability for Cu interconnects," *Mater. Sci. Semicond. Process.*, vol. 7, no. 3, pp. 157–163, 2004.

[16] M. Hauschildt *et al.*, "Large-scale statistical analysis of early failures in Cu electromigration, Part I: Dominating mechanisms," *J. Appl. Phys.*, vol. 108, no. 1, pp. 13 523–1–13 523–10, 2010.

[17] S. Alam *et al.*, "Circuit-level reliability requirements for Cu metallization," *IEEE T. Device Mater. Rel.*, vol. 5, no. 3, pp. 522–531, 2005.

[18] S. R. Nassif, "Power grid analysis benchmarks," in *Proc. ASP-DAC*, 2008, pp. 376–381.